Biocompatibility and Fatigue Properties of Polystyrene−Polyisobutylene−Polystyrene, an Emerging Thermoplastic Elastomeric Biomaterial

Miroslawa El Fray,[†] Piotr Prowans,[‡] Judit E. Puskas,*[,§] and Volker Altstädt[||]

Biomaterials and Functional Polymers Laboratory, Polymer Institute, Szczecin University of Technology, Pulaskiego 10, 70-322 Szczecin, Poland, General and Hand Surgery Clinic, Pomeranian Medical University, Unii Lubelskiej 1, Szczecin, Poland, Department of Polymer Science, The University of Akron, Akron, Ohio 44325, and Department of Polymer & Engineering, University of Bayreuth, Universitätsstr. 30, 95440 Bayreuth, Germany

Received December 19, 2005; Revised Manuscript Received January 18, 2006

This paper will discuss the biocompatibility and dynamic fatigue properties of polystyrene-*b*-polyisobutylene-*b*-polystyrene thermoplastic elastomer with 30 wt % polystyrene (SIBS30), an emerging FDA-approved biomaterial. SIBS30 is a very soft, transparent biomaterial resembling silicone rubber, with superior mechanical properties. Using the hysteresis method adopted for soft biomaterials, the dynamic fatigue properties of SIBS30 were found to be between those of polyurethane and silicone rubber, with fatigue life twice as long as that of silicone. Under single load testing (SLT, 1.25 MPa), SIBS30 displayed less than half the dynamic creep compared to silicone, both in air and in vitro (37 °C, simulated body fluid). Hemolysis and 30- and 180-day implantation studies revealed excellent biocompatibility of the new biomaterial. The results presented in this paper indicate that, in comparison with silicone rubber, SIBS30 has similar biocompatibility and superior dynamic fatigue properties.

Introduction

Polystyrene-*b*-polyisobutylene-*b*-polystyrene triblock copolymer with about 30 wt % polystyrene (SIBS30) is a new biomaterial.[1−7] It has been in clinical practice as the drug-eluting coating on the Taxus coronary stent under the trade name of Translute, which received FDA approval in 2004.[8] SIBS30 is a transparent material, categorized as a thermoplastic elastomer (TPE).[5] TPEs do not need to be vulcanized and therefore offer many advantages over chemically cross-linked rubbers, while being processible as classical thermoplastics. Figure 1 compares the network structure of SIBS30 (A−B−A type triblock) with $(A-B)_n$ type TPEs (polyesters or polyurethanes) and chemically cross-linked (thermoset) rubbers. Multiblock TPE polyesters and polyurethanes with similar network structures have long been used as biomaterials.[9−12] With Shore A > 100 hardness, medical-grade polyesters can hardly be considered elastomeric and are used in woven or knitted structures to yield increased flexibility. Polyurethane biomaterials are characterized by excellent mechanical and fatigue properties. However, they are subject to biodegradation; the in vivo hydrolysis of polyurethanes may lead to potentially toxic diamines.[12] In TPE biomaterials, microphase separation occurs because of the chemical incompatibility between the different blocks; the chemical structure of SIBS30 is shown in Figure 2a. SIBS30 has well-ordered nanostructure (see Figure 2b), while polyesters and polyurethanes have less-ordered nanophases. The hard blocks in polyurethanes are semicrystalline and are reinforced additionally by hydrogen bonding, which contributes to good fatigue properties. SIBS30 contains amorphous hard polystyrene blocks, and its segregated phase morphology leads to tensile properties equivalent to those of cross-linked and reinforced rubbers (thermosets).[5] Silicone rubbers are classified as "thermoset rubber".[13] They are based on poly(dimethylsiloxane), carrying functional groups for cross-linking (vulcanization) with peroxides or platinum, and are filled with silica to reinforce the weak cross-linked "gum" rubber (SIL). The exact chemical composition of medical-grade silicone rubber is usually proprietary; Figure 3 shows a general example. Reinforced medical-grade silicone rubber is still weak in comparison with other reinforced rubbers.[5,7,13] The unique stability of silicone rubbers in the biological environment has been a driving force for their continued use.

This work will report the results of biocompatibility studies and dynamic fatigue and creep testing of SIBS30 using the hysteresis method in air and in simulated body fluid (SBF) at 24 and 37 °C, and compare the results with those reported for selected polyester (PED26), polyurethane (PU), and silicone rubber (SIL) biomaterials.[14−16] Understanding the dynamic fatigue and creep properties of biomaterials designed for long-term implant applications is of great importance, since they are expected to remain structurally stable and durable under long-term cyclic loading. In general, two experimental strategies can be applied to investigate the fatigue properties of polymers: One originates from fracture mechanics and investigates flex cracking and crack growth behavior.[17] In the rubber industry, a typical example is the de Mattia flex fatigue test (ASTM D-813 and ASTM D-430). Since some materials such as styrene−butadiene rubber are resistant to cracking/failure due to flexing alone, crack initiation is recommended. This is close to real-life conditions where soft materials are exposed to small cuts. However, no correlation with actual service life is claimed in the procedure. The other strategy is the so-called hysteresis method,[18,19] which is less known and has just recently been applied to biomaterials,[14−16] including silicone rubber designed for optimum fatigue (tendon prosthesis). This method measures hysteresis

[†] Szczecin University of Technology.
[‡] Pomeranian Medical University.
[§] The University of Akron.
[||] University of Bayreuth.

10.1021/bm050971c CCC: $33.50
Published on Web 02/22/2006

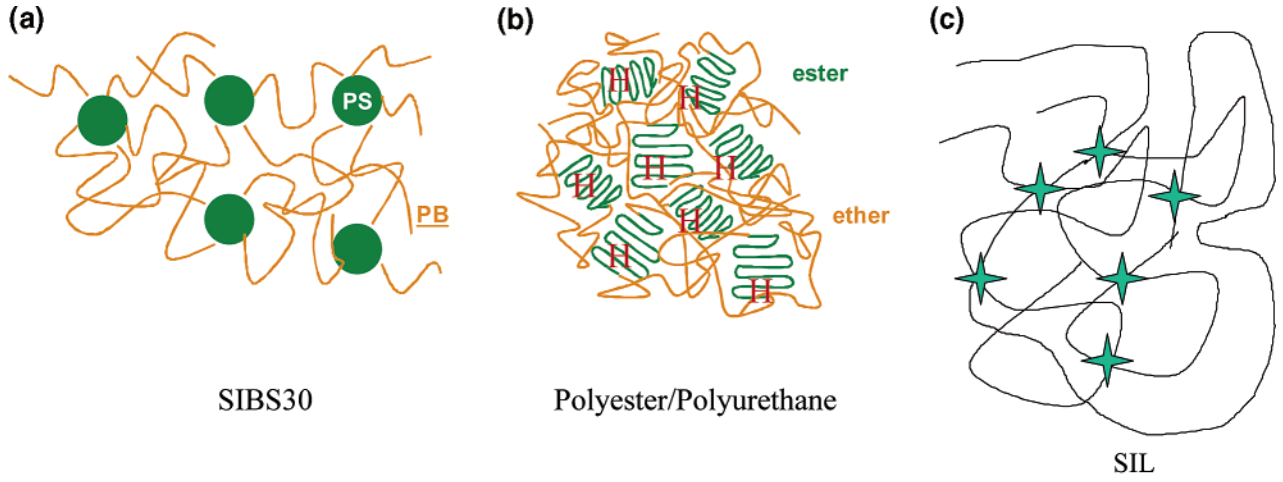

Figure 1. Schematics of the network structure of SIBS30 (a) in comparison with thermoplastic elastomer polyesters (b) and thermoset silicone rubber rubber (c).

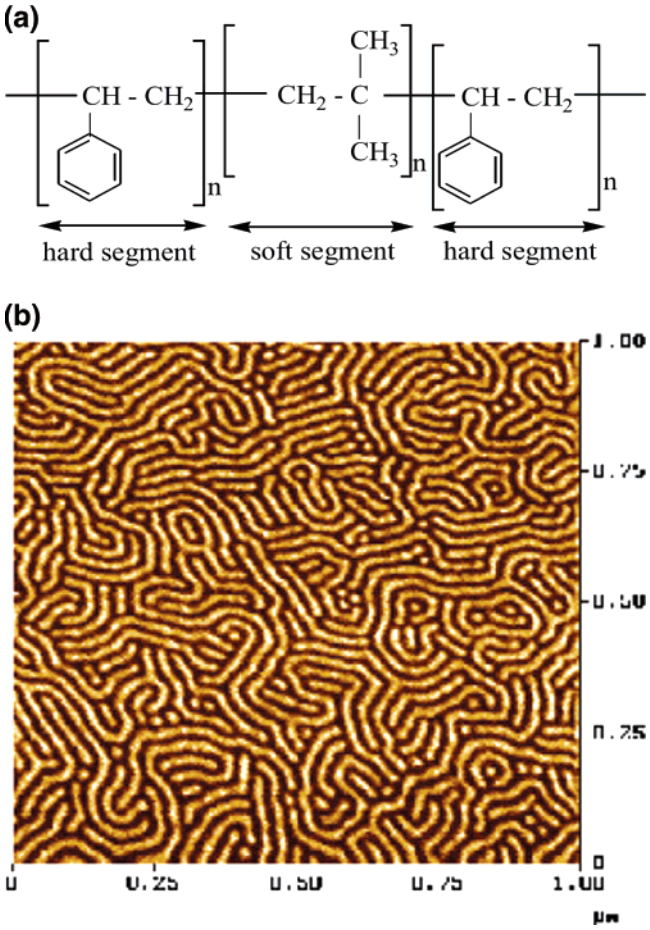

Figure 2. (a) Chemical structure and (b) AFM image of the phase morphology of SIBS30.

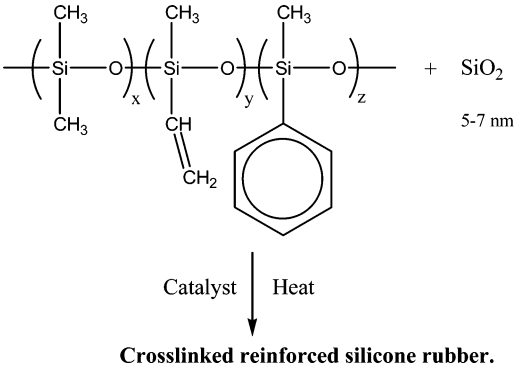

Figure 3. General chemical structure, cross-linking, and reinforcing of SIL.

loops under stress-controlled or strain-controlled conditions, and dynamic moduli are determined from the mid-curve intersecting the loops for equal strain or stress. Dynamic creep (dimensional change under cyclic stress) or dynamic stress relaxation (energy dissipation under cyclic strain) data can also be obtained from the loops. Since this method is not well-known and generated interest from polymer chemists working with biomaterials, a brief summary of the stress-controlled method to be used in this work will be presented here. First, the quasi-static tensile properties of the specimen are measured. Then, SILT (stepwise increasing load testing) is carried out to monitor dynamic modulus profiles. SILT stages are set in the range 5−50% of the ultimate tensile strength (UTS). At each step, dynamic loading is applied for a predetermined number of cycles. The phase shift between stress and strain is minimized, and the frequency is kept low (1−4 Hz) to avoid hysteretic heat generation. (Incidentally, this frequency range coincides with natural physiological frequencies occurring in the human body.) Dynamic creep is determined from SLT (single load testing). The load level for SLT is selected from the SILT profile, where the drop in dynamic modulus exceeds 5%. SLT then is carried out for a predetermined number of cycles, and dimensional changes are monitored. For biomaterial testing, SILT and SLT need to be carried out in air as well as in vitro (37 °C, simulated body fluid, SBF). It is well-known that fatigue failure in synthetic polymers is accelerated in the simultaneous presence of stress and liquids/solvents. The structural integrity of polymers designed for endoprostheses (i.e., in vivo long-term implants) can be compromised by fatigue failure under cyclic stress, assisted by corrosive physiological conditions. This was demonstrated in the case of cardiac valve prostheses made of glutaraldehyde and silicone-rubber-based tendon prostheses.[17,19,20]

This hysteresis method will be used to evaluate the dynamic fatigue and creep properties of SIBS30.

Experimental Section

Materials. A sample of commercially test-marketed SIBS30 (TS polymer, low MW type) with 30 wt % PS hard blocks, specific gravity

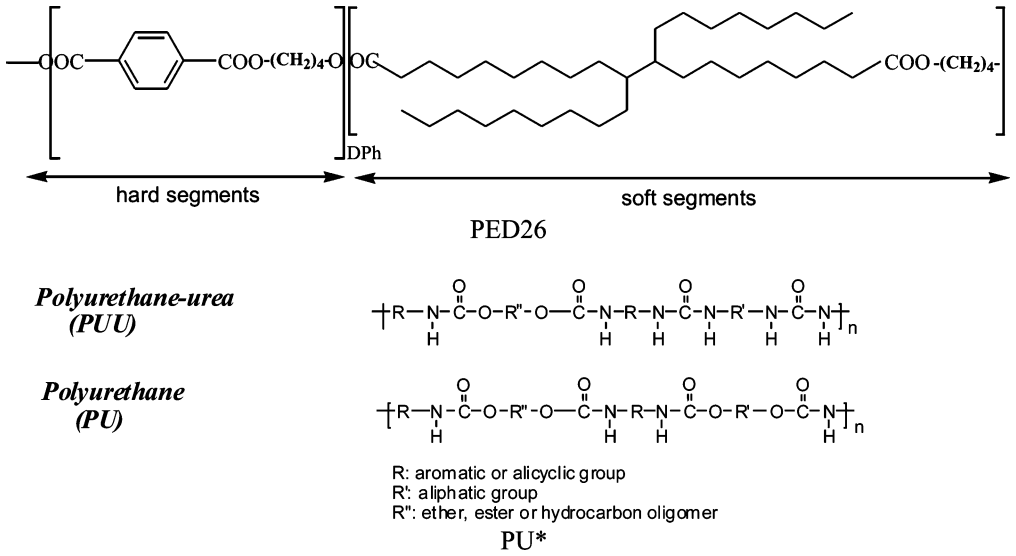

Figure 4. General chemical structures of (a) PED26 and (b) PU.

= 0.95 g/cm^3, JIS-A hardness = 56, tensile stress = 10.8 MPa with 440% elongation, and MFR (230 °C, 2.16 kg) = 5.8 g/10 min, was obtained by courtesy of Kuraray America, Inc., New York, a subsidiary of Kuraray Co., Ltd., Osaka, Japan. Its molecular weight (MW) and molecular weight distribution (MWD) were measured to be M_n = 60 000 g/mol and MWD = 1.56.[21] Silicone rubber (Mentor Medical System BV, The Netherlands) used in clinical practice as breast implant prostheses was used as a control for implantation tests. SBF was prepared as previously described.[20]

Procedures. *Sample Preparation.* For hemolysis and implantation, circular disks with 9 mm diameter and 1 mm thickness were die-cut from compression molded (150 °C at 8 MPa, 3 min) SIBS30 sheets. Silicone rubber disks of 9 mm diameter and 0.5 mm thickness were cut from the breast implant shell. S-2 dumbbells (3 mm thick with a cross-sectional area of 12 mm^2, ASTM D 1897-77) for tensile and fatigue testing were prepared by injection molding SIBS30 at 50 MPa pressure and 160 °C. The mold-lock pressure was 10 000 N, and the mold was kept at room temperature.

Hemolysis. The hemolysis tests were performed according to ASTM F756. Human and sheep red blood cells (5%) were suspended in trypted soy agar. *Streptococcal* clusters were used as control.

In vivo Biocompatibility. Ethylene oxide (EtO) sterilized SIBS30 and silicone rubber disks were implanted in the soft tissue of the abdominal wall and muscle tissue of male white mice weighing 18−20 g under aseptic conditions. The samples were retrieved from mice sacrificed after 30 and 180 days and were embedded in paraffin. Semithin (4−6 μm) sections were stained with hamatoxylin and eosin (HE) for cellular detail and morphology, and examined by light microscopy using a Leica Q600 Qwin image analyzer using a magnification of 200. Capsule thickness in direct contact with the polymer after 180 days was measured at 5 separate locations. The number of vessels (per capsule unit length) and the number of inflammatory cells were evaluated by counting at 3 random locations and a magnification of 400.

Tensile Testing. Quasi-static tensile data were collected at room temperature with an Instron 1161 tensile tester, equipped with a 500 N load cell, at a crosshead speed of 100 mm/min (ASTM D 638). Strain was measured by clamp displacement. The results reported are averaged for 6 specimens.

Fatigue Testing. Fatigue testing was carried out using a servo-hydraulic test machine with a digital controller (Instron 8400/8800), equipped with a 200 N load cell, a 10 kN cylinder and an environmental chamber (Figure 5). For all tests, the load ratio $R = \sigma_{min}/\sigma_{max}$ was held constant at 0.1. The strain was measured as the real-time clamp displacement. The possible phase shift between the stress and strain signals was minimized below 20 μs by the experimental setup. Testing in SBF was carried out at 24 and 37 °C; the temperature was controlled using a Lauda A100 pump. The DynMat Hysteresis Measurement Software V.1.1.0.1 (BASF AG) was used for the evaluation of the hysteresis loops.

Stepwise Increasing Load Test (SILT). Specimens were subjected to a stress-controlled sinusoidal oscillation with R = 0.1. The stress was kept constant for 1000 cycles before raising it to the next level. An interval of 100 cycles was implemented between every step to allow the controller to reach the higher loading level. The frequency of the cyclic loading was varied according to the stress levels: 5%, 10%, and 15% UTS − 4 Hz; 20%, 25%, and 30% − 3 Hz; 35% and 40% − 2 Hz; 45% and 50% − 1 Hz. The temperature of the samples was monitored with a thermocouple, and no hysteretic heating was observed.

Single Load Test (SLT). Specimens were subjected to a stress-controlled sinusoidal oscillation with 1 Hz frequency and R = 0.1. The maximum stress was set to a value determined from SILT as the load level where the drop in the dynamic modulus exceeded 5% (Table 2). STL was carried out for 100 000 cycles in air at 24 °C and for 36 000 cycles in the environmental chamber. The first 12 000 cycles were carried out in air at room temperature to establish a baseline, followed by 12 000 cycles in SBF at 24 °C before raising the temperature to 37 °C (24 000 to 36 000 cycles). The temperature of the samples was monitored, and no hysteretic heating was observed.

Results and Discussion

Hemolysis. SIBS30 was assessed to be nontoxic, since this material exhibited no hemolytic responses; the hemolytic indices were 0, in comparison with *Streptococcal* clusters that caused hemolysis. Figure 6 shows SIBS30 disks immersed in human and sheep red blood cells, with no visible reaction, while hemolytic activity was detected for two *Streptococcal* clusters (bottom of the Petri dish). After removal of the polymer disks from the agar/cells suspension, no sign of hemolysis was detected.

In Vivo Biocompatibility. Figure 7 demonstrates that, after 30 days implantation, no inflammation and minimal adverse tissue reaction to SIBS30 were found, similarly to the silicone control disks, thus demonstrating good biocompatibility of the polymer. Histological investigations confirmed the appearance of fibrous connective tissue enveloping the SIBS30 and silicone implants (Figure 7a,b; magnification 40×). Predominantly, granulocytes, lymphocytes, and a few fibroblasts were detected, which is considered a typical tissue response to the presence of

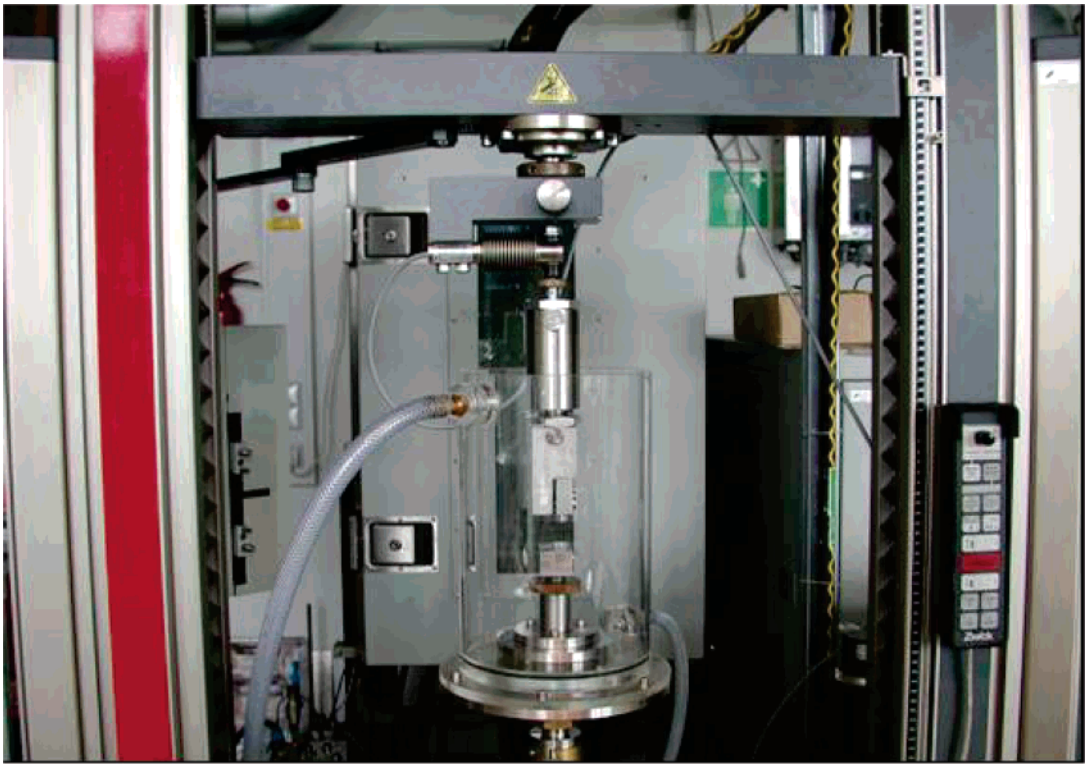

Figure 5. Environmental chamber for fatigue testing.

Table 1. Cell Count after Long-Term (180 days) Implantation[a]

cell type (number)	SIBS30	control	*p*
total inflammatory cells	18.93 ± 9.53	18.3 ± 9.23	0.97
lymphocytes	9.30 ± 7.21	9.96 ± 5.79	0.27
neutrophiles	3.70 ± 3.11	1.33 ± 2.53	0.0002
plasma cells	1.81 ± 2.11	4.81 ± 4.31	0.0001
eosinophiles	0.26 ± 0.56	0.78 ± 1.19	0.12
giant cells	0.70 ± 1.64	0 ± 0	
histiocytes	3.15 ± 3.35	1.75 ± 1.36	0.17

[a] Grading: 1+.[22]

Table 2. Quasi-Static Tensile Properties of SIBS30

sample code	σ_r (UTS) [MPa]	ϵ [%]	E_{mod} [MPa]	Shore A
SIBS30	5.6 ± 0.8 (8.0 ± 1.0*)	220 ± 10 (230 ± 11[a])	12 ± 1.7 (11 ± 2.3[a])	56

[a] Crosshead speed: 500 mm/min. σ_r = stress at break (ultimate tensile strength, UTS), ϵ = elongation at break, E_{mod} = Young's modulus.

a foreign body. The formation of a 0.1 mm thick fibrous capsule containing collagen fibers was observed, possibly the result of a nonspecific response by the tissue to the physical presence of the implant. The thickness of the fibrous layer found around the silicone implant was in the range 0.08−0.095 mm. The superiority of fibroblasts, the small number of granulocytes, and the lack of giant cells reflect a nonprotracted−nonspecific inflammatory reaction, indicating good biocompatibility of the tested polymeric materials. Long-term implantation (180 days) resulted in average compact capsule thicknesses of 47 and 21 μm for SIBS30 and the silicone control, respectively. The total numbers of inflammatory cells were comparable, as shown in Table 1, with more neutrophils (acute inflammation), but fewer plasma cells (chronic inflammation) for SIBS30. All cell counts fell into the lowest grade (+1) reported for biomaterials.[22] While these data support good biocompatibility, because of the limited number of samples they must be viewed with caution and more data need to be generated. The success of the Taxus stent in clinical practice, on the other hand, verifies excellent biocompatibility.[1,8]

The biocompatibility of SIBS30 most likely is related to the fact that the surface of SIBS30 is covered with a thin (10 nm) pure polyisobutylene layer, on account of the lower surface energy of the rubber phase. This was suggested first by Krausch et al. for block copolymers with polybutadiene rubber segments.[23] Subsequently. photoelectron spectroscopy (XPS) was used to verify this for SIBS30.[24] Thus, only polyisobutylene is in direct contact with biological tissues, while the polystyrene phases are buried within the material, providing reinforcement of the rubber phase; see Figure 8.

Dynamic Fatigue Properties. The quasi-static tensile properties of SIBS30 obtained with 100 and 500 mm/min crosshead speeds are listed in Table 2 (deviation from the nominal values listed in the Experimental Section is due to different testing conditions). Stepwise increasing load test (SILT) was carried out as described in the Experimental Section, and Figure 9 shows the change in dynamic modulus versus cycle number within each step. It was found that at each stress level the dynamic modulus, E_{dyn}, exponentially decreased, with a steady overall decline. SIBS30 failed around 10 000 cycles (40% UTS load). Equivalent SILT data for PED26, PU, and SIL published earlier[14,15] were plotted on the same graph. PED26 displays the smallest overall slope and failed at 12 000 cycles (50% UTS load). PU failed at about 10 000 cycles (40% UTS load). At failure, SIBS30 and PU have similar strengths (6−8 MPa). The difference in behavior can be explained in terms of differences in the chemical and network structures of the TPEs (SIBS30, PU, and PED26), shown in Figures 1, 3, and 4 (the exact structure of the commercial PU is unknown, so general structures are shown in Figure 4b). The structure of the TPEs is stabilized by physical cross-links (polystyrene glassy domains in SIBS30, crystalline ester domains in PED26, and urethane segments in PU). The much higher initial dynamic moduli values of the PU,

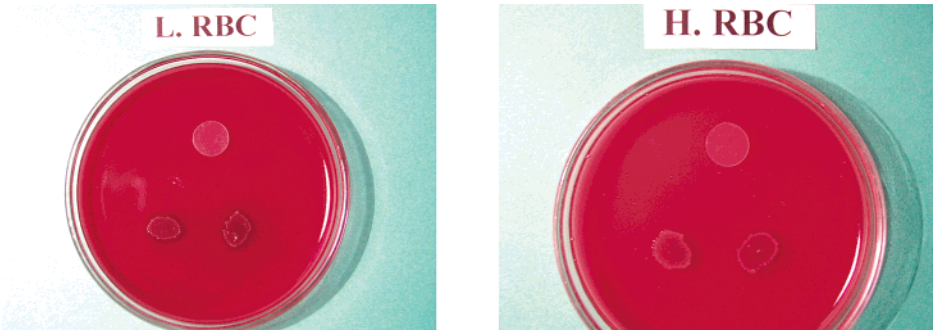

Figure 6. Hemolysis of SIBS. H.RBC − human red blood cells; L.RBC− sheep red blood cells (see text for detailed description).

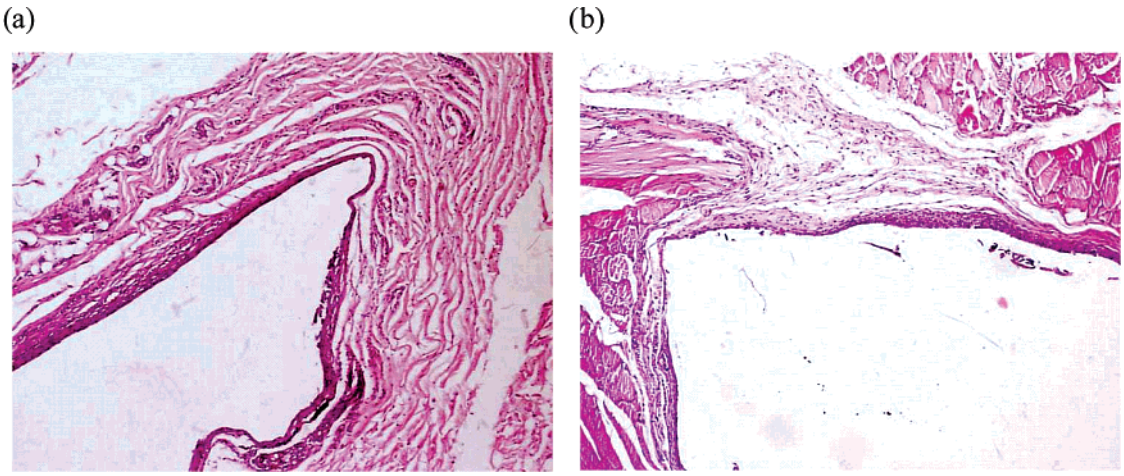

Figure 7. Histopathological slides of tissue around SIBS30 polymeric implant (a) and silicone control (b) (30 days of implantation).

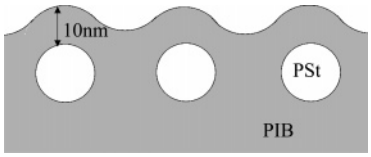

Figure 8. Surface topology of SIBS30.

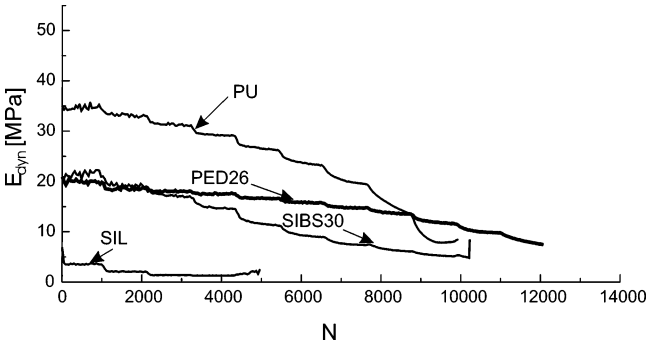

Figure 9. SILT: Dynamic moduli − cycle number profiles.

coupled with faster decrease, was interpreted by hydrogen bonding, but under cyclic deformation, destruction of the hard domains and/or intermixing of the hard and soft segments was observed.[14] SIBS30 has only amorphous hard domains, while PED26 has semicrystalline hard segments. In these terms, the best fatigue resistance of PED26 can be understood.[14,15] SIL shows a significantly different pattern in E_{dyn} change. Starting from an extremely low dynamic modulus, it failed at 5000 cycles (only 15% of its UTS). Such poor behavior in terms of dynamic modulus decrease and failure under cyclical loading may explain the premature failure of silicone rubber in load-bearing medical applications. Silicone rubber has been used in flexible joint prostheses in hand arthroplasty for many years[25,26] and is known to be susceptible to fracture. This susceptibility was usually explained by its relatively low tear strength,[27] but silicone rubber has relatively high tear strength in comparison with other rubbers. The testing methodology currently used for fatigue rupture testing of silicone breast implants showed that these devices should not rupture under loads well in excess of those expected in vivo. However, silicone breast implants are known to rupture in vivo, thus the validity of the current compression method was questioned by the FDA (Food and Drug Administration, U.S.A.).[28] We propose that the pattern in dynamic modulus change under oscillatory deformation, displayed in Figure 9, is a more important factor influencing the failure of silicone implants in load-bearing applications. In comparison, SIBS30 performed remarkably well, surviving twice as long as silicone rubber, despite its softness and amorphous structure.

Dynamic Creep Properties. The load for the single load test (SLT) for SIBS30 was determined to be 1.25 MPa. Figure 10 shows the dynamic creep profile in air at 24 °C. The instantaneous elastic deformation is 20%, which subsequently increases slowly and reaches about 30% at 100 000 cycles. At that point, the test was terminated. For comparison, the profiles published for PED26, PU, and SIL[14,15] are also shown in Figure 10, together with the load values (σ_{SLT}) used for the individual polymers. Thus, SIL was loaded only with 0.5 MPa, in comparison with 1.25 MPa for SIBS30 and PED26 and 2 MPa for PU: These values were determined from SILT as described in the Experimental Section. SIL shows 28% instantaneous elastic deformation—40% higher than SIBS at 4 times higher loading—but it remains practically constant up to 100 000 cycles. Both PU and PED26 display about 10% instantaneous elastic deformation, leveling off below 15% total deformation. The relatively small instantaneous deformation, coupled with moder-

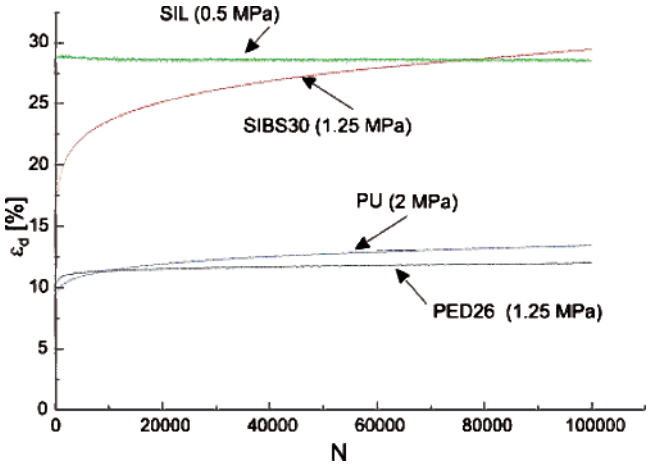

Figure 10. Dynamic creep plots for SIBS30, PED26, PU, and SIL. Test frequency: 1 Hz. N = number of cycles; T = 24 °C.

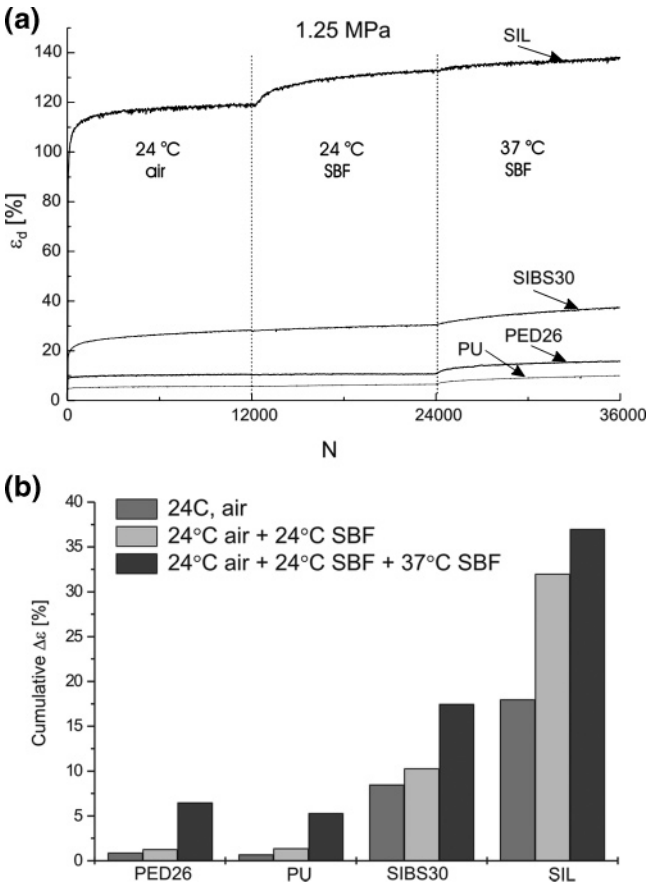

Figure 11. Comparison of the dynamic creep of SIBS30, PED26, PU, and SIL: (a) dynamic creep (ϵ) plots; (b) cumulative creep ($\Delta\epsilon$). σ SLT = 1.25 MPa. Test frequency: 1 Hz; 3 × 12 000 = 36 000 cycles.

ate creep, can be explained on the basis of the chemical and network structure of PED26 and PU (Figures 1 and 4) and the effective reinforcing of the hard segments (crystalline phases in PED26 and strong hydrogen bonds in PU). SIBS30 shows the highest creep, in line with its amorphous structure. The covalently cross-linked SIL (Figure 1) shows the smallest dynamic creep under the specified conditions. In contrast, testing with equal loading (1.25 MPa) reveals a different picture (Figure 11a). SIL shows tremendous instantaneous deformation of nearly 100% (5 times higher than SIBS30). Both show gradual creep until the end of the first 12 000 cycles (up to 24% and 120%). After the chamber is filled with SBF (middle stage in Figure 11a), SIBS30 creeps an additional 3% for the 12% of SIL. In the third phase (37 °C in SBF), SIBS30 has an additional 9% creep, compared to about 6% for SIL. The cumulative dynamic creep of SIBS30 is significantly lower than that of SIL (16% and 38%, respectively). Both PED26 and PU are quite resistant to dynamic creep in vitro (5−6%). Comparison of the dynamic creep behavior of SIBS30 with PED26, PU, and SIL can be seen in Figure 11b. The difference in behavior can be explained in terms of differences in the chemical structure of the TPEs as already discussed—crystalline phases and hydrogen bonding in PED26 and PU versus amorphous structure of SIBS30. The poor performance of covalently cross-linked and reinforced silicone was somewhat unexpected. At the same time, the findings presented here may explain the clinical experience of poor shape retention and rupture of silicone breast implant shells (both silicone gel and saline filled implants).[28] More research is needed to understand the underlying causes.

Conclusions

In our study, SIBS30 showed good biocompatibility, with no adverse biological effects. Its tissue response in 30- and 180-day implantation was similar to medical-grade silicone rubber. SIBS30 displayed superior fatigue properties in comparison with silicone, in air and in the presence of a simulated in vitro environment. The dynamic modulus of SIBS30 was measured to be 20 MPa, nearly 10 times higher than that reported for silicone rubber designed for tendon prosthesis. SIBS30 also had much better creep resistance in vitro (SBF, 37 °C). With the development of medical technology and the growth in artificial implants, there is a need for new biomaterials over a range of dynamic properties. SIBS30 is transparent and resembles medical-grade silicone rubber, but does not need reinforcing fillers and chemical cross-linkers. This, coupled with the excellent biocompatibility of SIBS30, predicts a bright future for this novel biomaterial. Preliminary experiments showed that the recently developed dendritic SIBS materials have even better dynamic fatigue and creep properties, because of their branched structure.[24,29,30]

Acknowledgment. Many thanks to the members of the Department of Polymer Engineering at the University of Bayreuth. Financial support by NSERC (Natural Sciences and Engineering Research Council of Canada), Lanxess Inc. (formerly Bayer Polymers (Bayer Inc., Canada)), DFG (Deutschen Forschunsgemeinschaft), the University of Akron, and NSF DMR Grant #0509687 is greatly appreciated. The authors are grateful to Dr. Sharon Grundfest-Broniatowski, Associate Professor of Surgery, Cleveland Clinic Lerner College of Medicine, and Dr. Stephen Schmidt and Michelle Chapman of Biomedical Research Associates Inc. for consultation.

Acknowledgment. A version of the fatigue testing part of this paper (#76) was presented at the 163rd Meeting of the Rubber Division of the American Chemical Society, Columbus, OH, October 5−8, 2004.

References and Notes

(1) Ranade, S. V.; Richard, R. E.; Helmus, M. N. Styrenic block copolymers for biomaterial and drug delivery applications. *Acta Biomater.* **2005**, *1*, 137−144.
(2) Kennedy, J. P.; Puskas, J. E.; Kaszas, G.; Hager, W. G. U.S. Patent 4,946,899, 1990.
(3) Pinchuk, L. (Corvita Corp., now Boston Scientific Inc.) U.S. Patent 5,741,331, 1998; U.S. Patent 6,102,939, 2000; U.S. Patent 6,197,240, 2001.

(4) Pinchuk, L.; Khan, I. J.; Martin, J. B.; Wilson, G. J. Polyisobutylene-Based Thermoplastic Elastomers for Ultra Long-Term Implant Applications; In *Sixth World Biomaterials Congress Transactions*; 2001; p 1452.
(5) Kennedy, J. P.; Puskas, J. E. In *Thermoplastic Elastomers*, 3rd ed.; Holden, G., Kricheldorf, H. R., Quirk, R., Eds.; Hanser Publishers: Munich, 2004; pp 285−321.
(6) Puskas, J. E.; Chen, Y.; Dahman, Y.; Padavan, D. Polyisobutylene-based biomaterials. *J. Polym. Sci., Part A: Polym. Chem.* **2004**, *42*, 3091−3109.
(7) Chen, Y.; Puskas, J. E. Polyisobutylene-based Thermoplastic Elastomers for Soft Tissue Replacement. *Biomacromolecules* **2004**, *5*, 1141−1154.
(8) *Taxus Express 2 Paclitaxel-Eluting Coronary Stent System (Monorail and Over the Wire)*; Publication PO30025; U.S. Food and Drug Administration; U.S. Government Printing Office: Washington, DC, 2004.
(9) Wise, D. L. *Biomaterials and Bioengineering Handbook*; Marcel Dekker: New York, 2000.
(10) Szycher, M. *Polyurethane Elastomers in Medicine*; Marcel Dekker: New York, 1990.
(11) Peppas, N. A.; Langer, R. New Challenges in Biomaterials. *Science* **1994**, *263*, 1715−1720.
(12) Pinchuk, L. *J. Biomater. Sci., Polym. Ed.* **1994**, *6* (3), 225.
(13) *Rubber Technology*; Morton, M., Ed.; Van Nostrand Reinhold Co.: New York, 1973.
(14) El Fray, M.; Altstädt, V. Fatigue behaviour of multiblock thermoplastic elastomers. 1. Stepwise increasing load testing of poly(aliphatic/aromatic-ester) copolymers. *Polymer* **2003**, *44*, 4635−4642.
(15) El Fray, M.; Altstädt, V. Fatigue behaviour of multiblock thermoplastic elastomers. 2. Dynamic creep of poly(aliphatic/aromatic-ester) copolymers. *Polymer* **2003**, *44*, 4643−4650.
(16) El Fray, M.; Altstädt, V. Fatigue behaviour of multiblock thermoplastic elastomers. 3. Stepwise increasing strain test of poly(aliphatic/aromatic-ester) copolymers. *Polymer* **2004**, *45*, 263−273.
(17) Ritchie, R. O.; Dauskart, R. H.; Yu, W.; Brendzel, A. M. Cyclic fatigue-crack propagation, stress-corrosion, and fracture-toughness behavior in pyrolytic carbon-coated graphite for prosthetic heart valve applications. *J. Biomed. Mater. Res.* **1990**, *24*, 189−206.
(18) Renz, R.; Altstädt, V.; Ehrenstein, G. W. Hysteresis Measurements for Characterizing the Dynamic Fatigue of R-SMC. *J. Reinf. Plast. Compos.* **1988**, *7*, 413−434.
(19) Ward, T. C.; Perry, J. T. Dynamic mechanical properties of medical grade silicone elastomer stored in simulated body fluids. *J. Biomed. Mater. Res.* **1981**, *15*, 511−525.
(20) Renke-Gluszko, M.; El Fray, M. The effect of simulated body fluid on mechanical properties of multiblock poly(aliphatic/aromatic-ester) copolymers. *Biomaterials* **2004**, *25*, 5191−5198.
(21) Puskas, J. E.; Antony, P.; El Fray, M.; Altstädt, V. The effect of hard and soft segment composition and molecular architecture on the morphology and mechanical properties of polystyrene-polyisobutylene thermoplastic elastomeric block copolymers. *Eur. Polym. J.* **2003**, *39*, 2041−2049.
(22) Black, J. *Biological performance of materials*; Marcel Dekker: New York, 1999.
(23) Knoll, A.; Magerle, R.; Krausch, G. *Macromolecules* **2001**, *34*, 4159−4165.
(24) Puskas, J. E.; Kwon, Y.; Prince, A.; Bhowmick, A. K. Synthesis and Characterization of Novel Dendritic (Arborescent) Polyisobutylene-Polystyrene Thermoplastic Elastomers. *J. Polym. Sci., Part A: Polym. Chem.* **2004**, *43* (9), 1811−1826; cover page (2005).
(25) Blair, W. F.; Shurr, D. G.; Buckwalter, A. J. Metacarpophalangeal joint implant arthroplasty with a Silastic spacer. *J. Bone Joint Surg. Am.* **1984**, *66A*, 365−370.
(26) Vahvanen, V.; Viljakka, T. Silicone-rubber implant arthroplasty of the metacarpophalangeal joint in rheumatoid-arthritis − a follow-up-study of 32 patients. *J. Hand Surg. Am.* **1986**, *11A*, 333−339.
(27) Bieber, E. J.; Weiland, A. J.; Volenec-Dowling, S. Silicone-rubber implant arthroplasty of the metacarpophalangeal joints for rheumatoid arthritis. *J. Bone Joint Surg. Am.* **1986**, *68A*, 206−209.
(28) *Draft Guidance for Industry and FDA Staff: Saline, Silicone Gel and Alternative Breast Implants*; U.S. Food and Drug Admininstration; U.S. Government Printing Office: Washington, DC, January 13, 2004.
(29) Puskas, J. E.; Paulo, C.; Antony, P. U.S. Patent 6,747,098, 2004.
(30) Puskas, J. E.; Chen, Y.; Dahman, Y.; Padavan, D. Polyisobutylene-based biomaterials. *J. Polym. Sci., Part A: Polym. Chem.* **2004**, *42*, 3091−3109.

BM050971C